Supporting Information

Boric Acid Assisted Reduction of Graphene Oxide: A Promising Material for Sodium-ion Batteries

Ying Wang,[1,4] Caiyun Wang,[3] Yijing Wang,[2] Huakun Liu,[4] Zhenguo Huang[4*]*

[1]School of Chemistry and Chemical Engineering, Jiangsu Key Laboratory of Green Synthetic Chemistry for Functional Materials, Jiangsu Normal University, Xuzhou, Jiangsu 221116, China.

[2]Collaborative Innovation Centre of Chemical Science and Engineering (Tianjin), Key Laboratory of Advanced Energy Materials Chemistry (MOE), Nankai University, Tianjin 300071, China. E-mail: wangyj@nankai.edu.cn

[3]Intelligent Polymer Research Institute, ARC Centre of Excellence for Electromaterials Science, University of Wollongong, Wollongong, NSW 2522, Australia.

[4]Institute for Superconducting and Electronic Materials, University of Wollongong, Wollongong, NSW 2522, Australia. E-mail: zhenguo@uow.edu.au.

1. Characterization

X-ray diffraction (XRD, GBC eMMA, Cu Kα radiation, λ = 1.5406 Å), X-ray photoelectron spectroscopy (XPS, VG Scientific ESCALAB 2201XL, Al Kα X-ray radiation), Fourier transform infrared spectroscopy (FTIR, Shimadzu Prestige-21), nitrogen-sorption isothermal analysis (NOVA 2200e, Quantachrome), and Raman spectroscopy (Jobin Yvon HR800 Raman spectrometer with a 10 mW helium/neon laser at 632.8 nm excitation) were used to determine the structure and composition of samples. Scanning electron microscopy (SEM, JEOL JSM7500FA), transmission electron microscopy (TEM), and high-resolution TEM (HR-TEM, JEOL JEM-2010FEF) were used for morphological investigations.

2. Electrochemical measurements

The electrochemical performances were evaluated by using standard 2032 type coin cells. The working electrodes were fabricated with 80 wt% active materials, 10 wt% acetylene black (Super P), and 10 wt% sodium carboxymethyl cellulose (CMC) in deionized water to form a slurry, which was then cast onto copper foil and dried in dynamic vacuum at 60 °C overnight. Higher temperatures could cause further dehydration in BF-rGO and consequently, an unwanted smaller interlayer spacing. A sodium disc was used as the counter electrode. The electrodes were separated by glass fiber. Electrolytes consisting of1 M $NaClO_4$ in three different solvents were used to optimize the electrochemical performance: (1) 1,2-dimethoxyethane (DME); (2) ethylene carbonate (EC) and diethyl carbonate (DEC) (EC:DEC, 1:1, v:v); (3) EC:DEC with the addition of 5 % fluorinated ethylene carbonate (FEC) (EC:DEC:FEC). The cells were assembled in an argon filled glove box with the oxygen and water content below 1 ppm. Galvanostatic charge-discharge tests were carried out on a

battery testing system (Shenzhen NEWARE Battery, China) in the voltage range between 0.001 and 2.00 V. Electrochemical impedance spectroscopy (EIS) measurements were performed on a Biologic VMP-3 electrochemical workstation. The capacity was calculated based on the active materials.

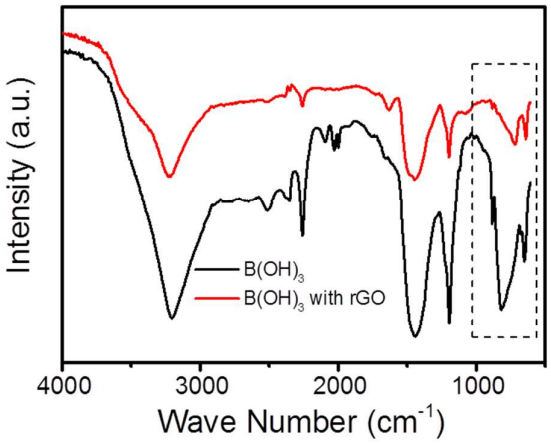

Figure S1 FTIR spectra of boric acid and freeze-dried mixture of boric acid and GO. The rectangle part shows the red shift of B−O−H out-of-plane bending, and O−B−O ring bending.

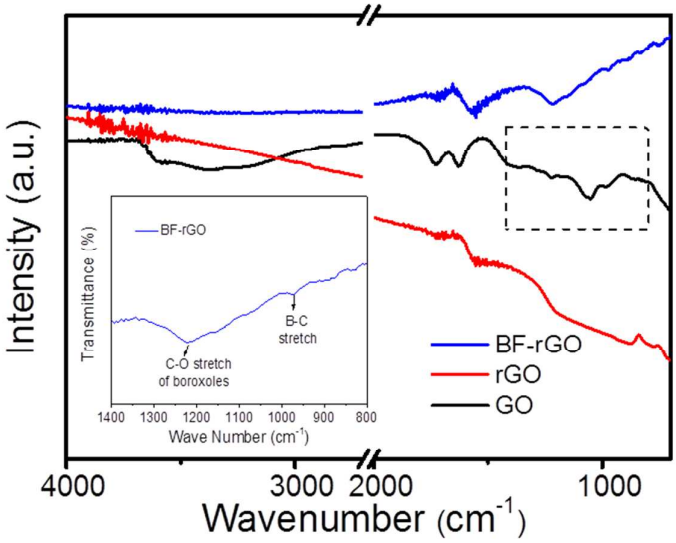

Figure S2 FTIR spectra of the GO, rGO, and BF-rGO samples. Inset is an enlargement of the dashed rectangle. After the reduction, most of the oxygen-containing groups in GO disappeared. The appearance of two peaks in the BF-rGO sample at 1215 and 968 cm^{-1} indicates the formation of C−O−B and C−B bonds, respectively.

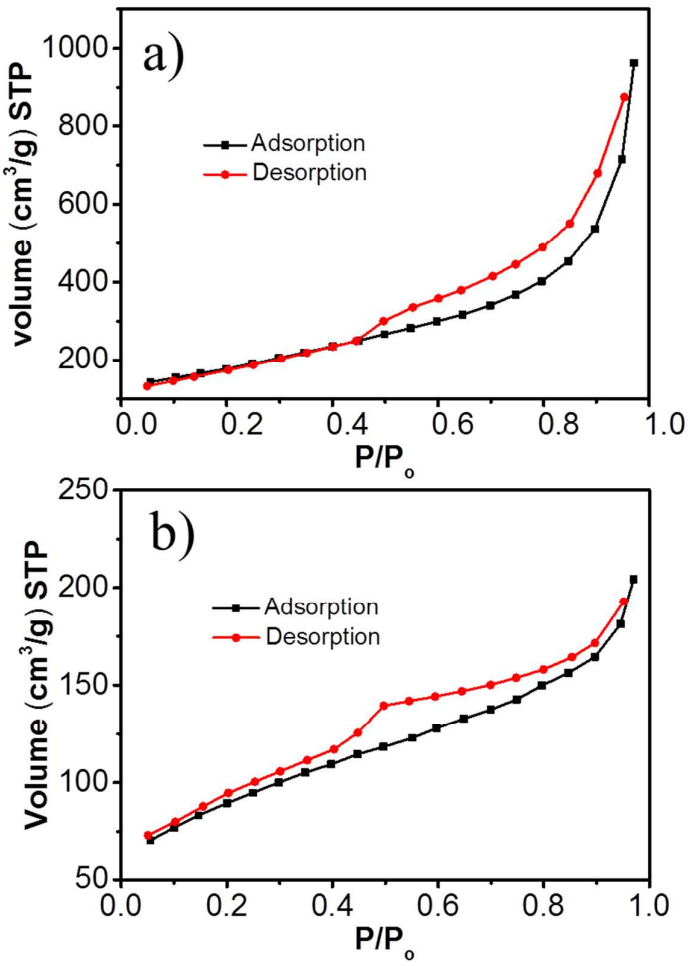

Figure S3 Nitrogen adsorption and desorption isotherms of (a) the pure rGO and (b) the as-obtained BF-rGO. The decreased surface area of the BF-rGO indicates the successful functionlization of rGO.

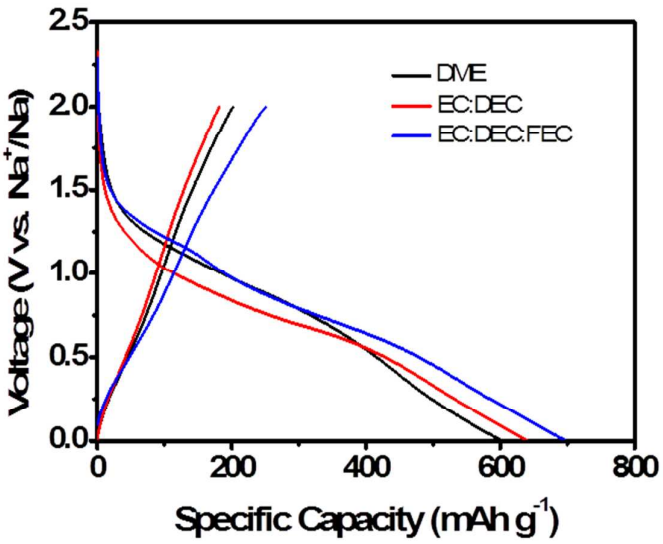

Figure S4 First cycle discharge-charge profiles for the BF-rGO/Na half cells in different electrolytes.

Table S1 Specific capacity for selected cycles of the Na/BF-rGO half cells.

Electrolyte	Capacity ($mAh \cdot g^{-1}$)				
	1^{st}	2^{nd}	5^{th}	10^{th}	115^{th}
DME	601	212	189	173	142
EC:DEC	640	191	168	159	128
EC:DEC:FEC	685	239	183	182	180

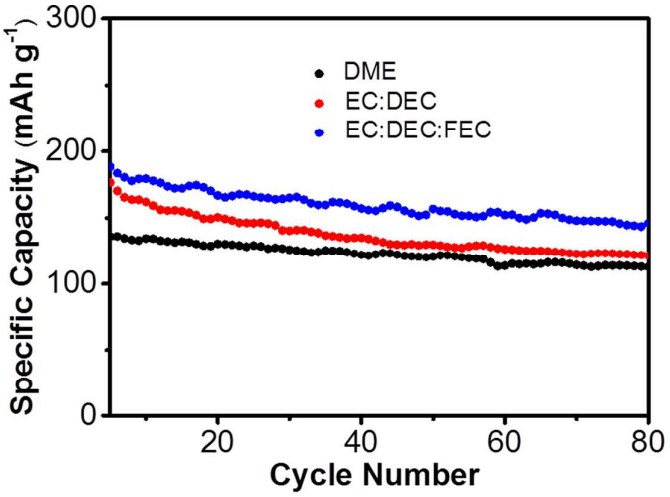

Figure S5 Cycling stability of the pure rGO electrode in different electrolytes.

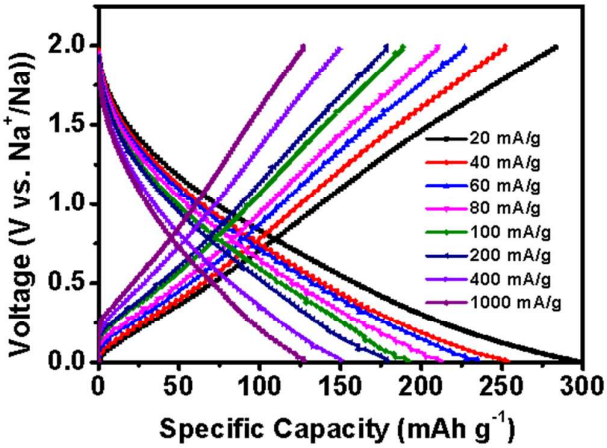

Figure S6 Discharge-charge curves of the Na/BF-rGO half cells at different current density.

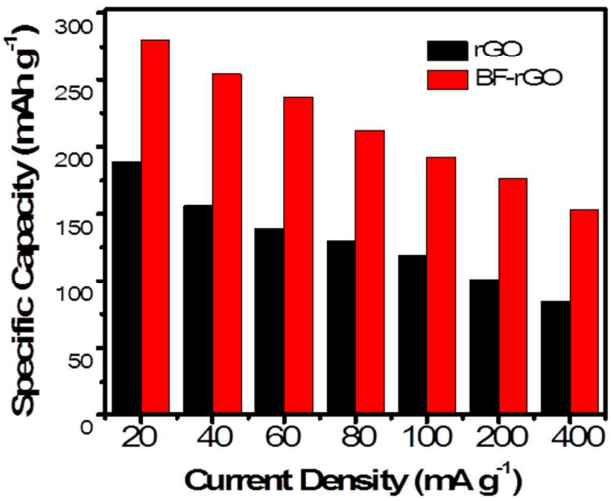

Figure S7 Rate capability of Na/rGO and Na/BF-rGO half cells.

Table S2 Parameters used to fit the Nyquist plots.

Sample	R_S	CPE-T	CPE-P	R_{ct}	W_o-R	W_o-T	W_o-P
rGO	30	1.8×10^{-6}	0.9	1509	22246	104.5	0.46
BF-rGO	10.5	4.5×10^{-6}	0.8	586	10487	25	0.31

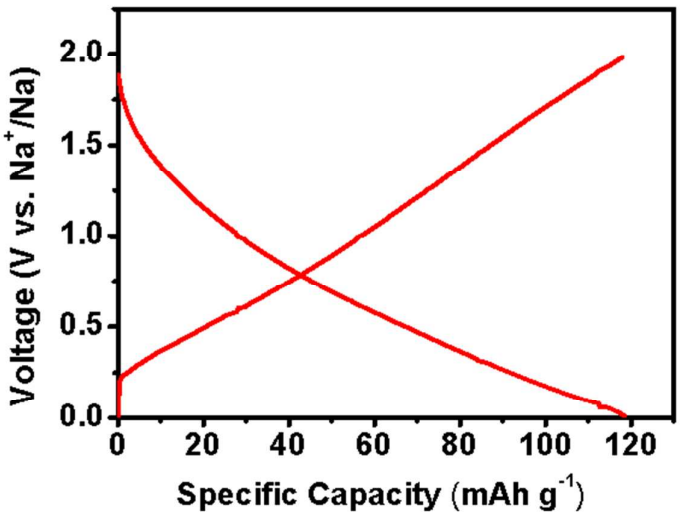

Figure S8 Discharge/charge voltage profile for the BF-rGO electrode after 5000 cycles.

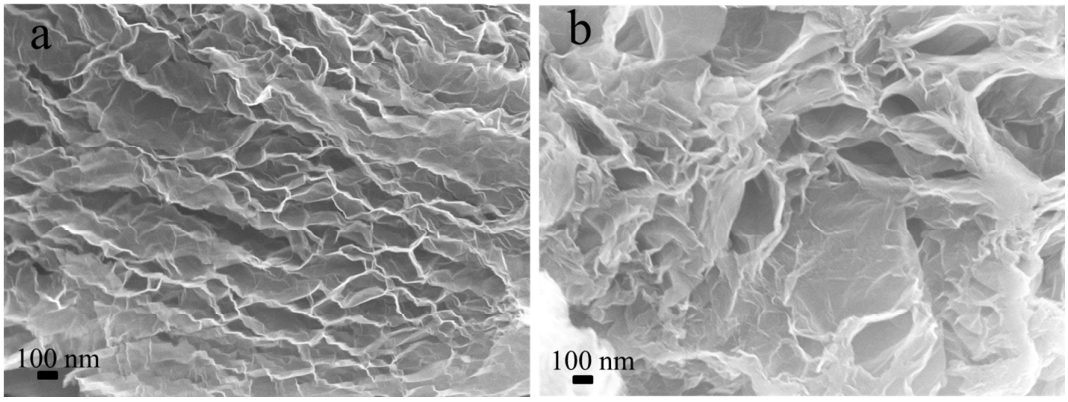

Figure S9 SEM images of (a) rGO and (b) BF-rGO.